ACS OMEGA

http://pubs.acs.org/journal/acsodf
Article

Adsorption Characteristics of Organic Pollutants on Montmorillonites Modified by Quaternary Ammonium Surfactants with Organic Counterions

Runyu Cao, Bowen Guan, Siqi Hu, Xinru Jia, Hongqin Liu,* and Baocai Xu

Cite This: *ACS Omega* 2025, 10, 10926−10937
Read Online

ACCESS | Metrics & More | Article Recommendations | Supporting Information

ABSTRACT: Na-montmorillonite (Na-Mt) modified by quaternary ammonium surfactants containing different organic counterions [OMt-QAS·Y^-, Y = $CH_3CO_3^-$, $CH_3(CH_2)_3COO^-$, $CH_3CH(OH)COO^-$, and $HCOO^-$] was prepared for enhancing the adsorption capacity of 2, 4-dichlorophenol/cibacron brilliant yellow 3G-P. Compared with Na-Mt, whose adsorption efficiency for 2,4-dichlorophenol/cibacron brilliant yellow 3G-P was only 58/1.85 mg/g, the adsorption efficiency of OMt-QAS·Y^- was greatly improved, with OMt-QAS·$CH_3CO_3^-$ having the highest adsorption capacity of 152.85/116.17 mg/g. The kinetic and isotherm studies indicate that all adsorption processes fit well to the pseudo-second-order model and Freundlich model, respectively. The hydrophobicity of counterions and their affinity with the aliphatic chains had an effect on the interlayer spacing and point of zero charge of OMt-QAS·Y^-, which in turn affected their adsorption properties.

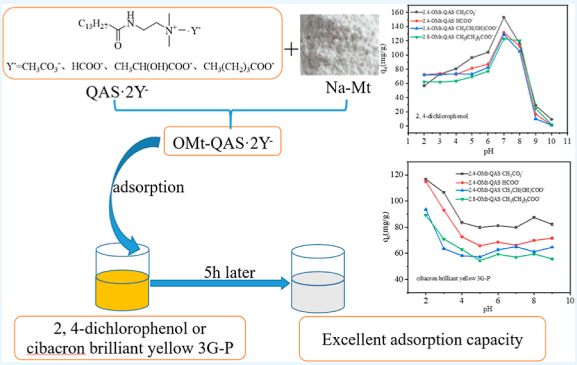

1. INTRODUCTION

In recent years, there has been a global focus on removing harmful substances from wastewater, including various phenolic pollutants and organic dyes, the concentration of which is generally tens to hundreds of mg/L. Chlorophenol are common environmental pollutants, mainly derived from pharmaceuticals, fungicides, preservatives, herbicides, insecticides, etc., and widely exist in environmental waters and soil.[1−6] Even at very low concentrations, they will produce toxic gases that adversely affect organisms.[7] The United States Environmental Protection Agency (EPA) has designated chlorophenol as a priority pollutant due to its potential carcinogenicity and mutagenicity. Azo dyes also widely exist in many industries such as textiles, leather, paper making, printing, cosmetics, etc.[8−11] Azo dyes give industrial wastewater its color, which can not only affect aquatic organisms by reducing sunlight penetration and light cooperation in aquatic flora but can also cause human skin problems and even carcinogenicity in many cases.[12] In recent years, various technologies such as distillation, adsorption, oxidation, enzymolysis, and biodegradation, etc. have been developed to remove these organic pollutants from industrial wastewater.[13−16] Among these, adsorption is an economical, efficient, relatively environmentally friendly and simple method, which is widely considered to be one of the most effective treatment methods for phenolic pollutants and organic dyes in wastewater.[17] Currently, the research and development of environmentally safe, efficient, and low-cost adsorbents for the elimination of various pollutants from wastewater has attracted widespread attention due to environmental and economic considerations.

Naturel clay minerals are low-cost, readily available, widely distributed, naturally occurring, and nontoxic. Due to their porous structure, large specific surface area, excellent cation exchange capacity (CEC), and high adsorption performance, they have attracted much attention as effective adsorbents for the adsorption of inorganic and organic pollutants in wastewater.[18] Natural Mt, one of the most commonly used clay in the treatment of wastewater, is hydrated sodium calcium aluminum magnesium silicate hydroxide $(Na, Ca)_x(Al, Mg)_2Si_4O_{10}(OH)_2{\cdot}nH_2O$ characterized by one Al octahedral sheet sandwiched between two Si tetrahedral sheets.[19] Nevertheless, the capacity of Mt to absorb organic pollutants is constrained by its low organic content and poor hydrophobicity.[20] It is noteworthy that Mt exhibits isomorphous substitution, whereby organic cations can replace compensating cations between clay mineral layers, resulting in organic intercalation. Consequently, through intermolecular interactions or ion exchange, cationic surfactants, in particular

Received: September 30, 2024
Revised: February 26, 2025
Accepted: March 4, 2025
Published: March 11, 2025

quaternary ammonium surfactants, can be employed to modify Mt. This process significantly increases the hydrophobicity and interlayer spacing of Mt, thereby enhancing the adsorption efficacy of organic pollutants.[18]

To date, numerous published reports have concentrated on studying the impact of the structural characteristics of quaternary ammonium surfactants with halogen ions (Br^-, Cl^-, and I^-) as counterions, including spacers, hydrophobic chains, and headgroups, on the interlayer environment and adsorption properties of modified Mt.[21−24] However, when the Mt modified with quaternary ammonium surfactant containing halogen ions is used to adsorb anionic pollutants, the charge-balanced halogen ions are released into the water medium treated with ion exchange, resulting in secondary pollution.[25] Moreover, studies have shown that counterions have a very significant effect on the micellar performance of quaternary ammonium surfactants. The effect of counterions on micellization properties cannot be described as the result of one single parameter of ions, but rather the equilibrium effects synergistically affect the propensity of counterions to form ion pairs with surfactant headgroups as well as the entropy gain upon micellization.[26] However, to the best of our knowledge, there have been few studies on the effect of counterions of quaternary ammonium surfactants on the adsorption properties of modified Mt.[27]

Therefore, in this study, we have prepared quaternary ammonium surfactants with different organic counterions for modifying Mt and studied their adsorption properties for 2, 4-dichlorophenol and cibacron brilliant yellow 3G-P. The impact of various factors, including organic counterions, surfactant amount, the dosage of OMt-QAS·Y^-, and the pH of the solution, on the adsorption performance is examined in depth. The adsorption mechanism for 2,4-dichlorophenol/cibacron brilliant yellow 3G-P is proposed on the basis of the structural characterizations, adsorption equilibrium isotherms, and adsorption kinetic models of OMts.

2. EXPERIMENTAL METHODS

2.1. Materials. Na-montmorillonite (Na-Mt) was provided by Beijing Inokai Technology Co., Ltd., China. The main elemental composition of Na-Mt was as follows (Wt %): Si 48.06, Al 9.89, Mg 3.04, Na 1.59, Ca 1.38, O 34.92, and C 1.12. Its CEC was 60 mmol/100 g. 2,4-Dichlorophenol (98%) was supplied by Shanghai Aladdin Biochemical Technology Co., Ltd., and cibacron brilliant yellow 3G-P (98%) was purchased from Shanghai Yuanye Biotechnology Co., Ltd. Ethanol (99.7%) was purchased from Sinopharm Chemical Reagent Co., Ltd. High purity water (ρ = 18.25 MΩ·cm^{-1}) was obtained from the ultrapure laboratory water purification system. The four quaternary ammonium surfactants with different organic counterions [QAS·Y^-, Y = $CH_3CO_3^-$, $HCOO^-$, $CH_3CH(OH)COO^-$, and $CH_3(CH_2)_3COO^-$], the chemical structure of which is shown in Figure 1, were synthesized according to our previous work.[28,29] The synthesis route of these compounds is given in the Supporting Information.

2.2. Surface Tension Measurements. The surface tension of the aqueous solution with the QAS·Y^- concentration range of 1×10^{-6} to 1×10^{-1} mol·L^{-1} was determined utilizing the Wilhemy plate method on the Delta8 surface tension meter in Kibron, Finland at 298.15 K. The surface tension was the average of the three measurements with a standard deviation of less than 0.02.

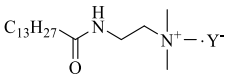

Y^-=$CH_3CO_3^-$、$HCOO^-$、$CH_3CH(OH)COO^-$、$CH_3(CH_2)_3COO^-$

Figure 1. Chemical structure of QAS·Y^-.

2.3. Preparation of Organic Mt (OMt). 2.0 g portion of Na-Mt was dispersed in 100 mL of deionized water with constant stirring until completely dispersed. The corresponding mass of QAS·Y^-, m_s (g), calculated according to eq 1, was added to another 100 mL of deionized water.

$$m_s = n \times \mathrm{CEC} \times M \times m_0 \quad (1)$$

In eq 1, n represents the multiple of the CEC of Na-Mt (mmol/g), m_0 (g) is the mass of Na-Mt, and M (g/mol) is the relative molecular weight of QAS·Y^-. The prepared modifier solution was then added to the Na-Mt suspension. The mixture was sealed and stirred at room temperature for 24 h. After that, the solution was filtered and the solid was leached with a large volume of high pure water until the surface tension of the clear liquid below was equal to that of the high pure water.

The obtained solid product was then dried in a hot blast furnace at 80 °C for 24 h. The dried organic Mt modified with QAS·Y^- was ground into powder in an agate mill, sieved through a 200-mesh sieve and labeled with n-OMt-QAS·Y^-.

2.4. Characterization of OMt. A Nicolet IS10 FT-IR spectrometer (Thermo Fisher) was employed to record FTIR spectra of samples in the range of 4000−400 cm^{-1} with a resolution of 4 cm^{-1}. The XRD patterns of Na-Mt and OMts were recorded using an X-ray diffractometer (Rigaku + UltimaIV) with a Cu Kα target radiation (λ = 0.154, 2θ = 2−10°, scanning speed = 1°/min). Thermogravimetric analysis was conducted on a METTLER TGA/DSC3+ thermogravimetric analyzer. The samples were heated in a flow of high purity nitrogen gas, with the temperature rising from 40 to 900 °C at a rate of 20 °C/min. The specific surface area and pore diameter analyzer (V-Sorb 2800) was employed to measure and calculate the specific surface area, total void volume, and average void radius of Na-Mt and OMts, utilizing the Brunauer, Emmett, and Teller (BET) method.

2.5. Adsorption Experiments. These four kinds of OMts were applied to absorb 2,4-dichlorophenol/cibacron brilliant yellow 3G-P. A comprehensive investigation was conducted into the influence of various parameters, including the dosage of modifier QAS·Y^-, OMt dosage, adsorption temperature and time, and solution pH. To ensure the reliability and reproducibility of the results, all experiments were repeated three times.

In order to determine the optimum amount of modifier, 0.04 g of OMt modified with different doses of QAS·Y^- was dispersed in 2, 4-dichlorophenol (or cibacron brilliant yellow 3G-P) solution and sealed. Then, each dispersion was filtered through a 0.45 μm membrane filter after oscillation for 6 h at 25 °C. After that, an UV−visible spectrophotometer (UV-3600, SHIMADZU, Japan) was used to determine the concentration of the residual 2,4-dichlophenol at 284 nm (pH = 2−7) or 304 nm (pH = 8−10) and the concentration of the residual cibacron brilliant yellow 3G-P at 266 nm. The adsorption capacity of OMt for 2,4-dichlorophenol/cibacron brilliant yellow 3G-P, q_e (mg/g), was calculated by the following equation

https://doi.org/10.1021/acsomega.4c08924
ACS Omega 2025, 10, 10926−10937

$$q_e = \frac{(C_0 - C_e) \times V}{m} \quad (2)$$

where c_0 (mg/L) and c_e (mg/L) were the initial and equilibrium concentrations of 2,4-dichlorophenol/cibacron brilliant yellow 3G-P, respectively, v (L) was the volume of the solution, and m (g) was the mass of OMt.

To determine the optimum amount of adsorbent addition, a series of addition experiments were conducted, in which different amounts of OMt-QAS·Y^- modified at 2.4 or 2.8 CEC were added into a solution of 2, 4-dichlorophenol/cibacron brilliant yellow 3G-P and oscillated for 6 h at 25 °C, respectively.

To investigate the effect of pH of the aqueous phase, the adsorption experiments were conducted in the pH range of 2−10 adjusted by 0.1 mol/L HCl or NaOH solution. At the same time, the point of zero charge (PZC) of OMt-QAS·Y^- was determined. First, 0.15 g of OMt-QAS·Y^- was introduced to 0.01 M NaCl solutions with a pH 2−11 adjusted by 0.1 mol/L HCl or NaOH solutions. After the mixture was stirred for 48 h, the final pH of these solutions was determined.

In all of the adsorption experiments, the initial concentration of 2,4-dichlorophenol/cibacron brilliant yellow 3G-P solution was 100 mg/L, and the volume was 100 mL. In addition, except for the experiments to investigate the effect of solution pH on the adsorption properties of OMts, the working pH of the other experiments is about 6.

2.6. Adsorption Kinetic Studies. 0.04 g of OMt-QAS·Y^- modified at 2.4 or 2.8 CEC was added into 100 mL of 2, 4-dichlorophenol/cibacron brilliant yellow 3G-P solution at a concentration of 100 mg/L and oscillated for 7 h at 25, 35, and 45 °C, respectively. Aliquots of the reaction solution were quickly taken at regular intervals and assayed. Subsequently, the pseudo-first-order (eq 3), pseudo-second-order (eq 4), and intraparticle diffusion models (eq 5) were employed to fit the experimental data to study the mechanism of adsorption and predict the adsorption kinetics[30]

$$\ln(q_e - q_t) = \ln q_e - k_1 t \quad (3)$$

$$\frac{t}{q_t} = \frac{1}{k_2 q_e^2} + \frac{t}{q_e} \quad (4)$$

$$q_t = k_p t^{1/2} + C \quad (5)$$

where q_e (mg/g) and q_t (mg/g) were the amount of 2,4-dichlorophenol/cibacron brilliant yellow 3G-P adsorbed by OMts at equilibrium and time t (min), k_1 (g/(mg·min) $^{-1}$), k_2 (g/(mg·min) $^{-1}$), and k_p (mg/g·$min^{1/2}$) stood for the adsorption rate constants, and the constant C provided insight into the thickness of the boundary layer.

2.7. Adsorption Isotherms Studies. To further understand the adsorption mechanism of 2,4-dichlorophenol/cibacron brilliant yellow 3G-P on OMts, Freundlich (eq 6) and Langmuir (eq 7) models were employed[31]

$$\ln q_e = \ln K_F + \frac{\ln C_e}{n} \quad (6)$$

$$\frac{C_e}{q_e} = \frac{1}{q_{max} K_L} + \frac{C_e}{q_{max}} \quad (7)$$

where q_{max} (mg/g) was the maximum adsorption capacity, K_F and n were the Freundlich constants, and K_L (L/mg) was the Langmuir constant.

2.8. Adsorption Thermodynamic Studies. In order to gain insight into the internal energy changes during adsorption, Gibbs free energy change (ΔG°), enthalpy change (ΔH°), and entropy change (ΔS°) were calculated according to eqs 8 and 9

$$\ln K = \Delta S^\circ/\mathrm{R} - \Delta H^\circ/(RT) \quad (8)$$

$$\Delta G^\circ = \Delta H^\circ - T\Delta S^\circ \quad (9)$$

where K (q_e/c_e) represented the distribution coefficient, R was the gas constant, and T denoted the absolute temperature. The values of ΔH° and ΔS° were derived from the intercepts and slopes of the linear plots of ln K versus $1/T$.

2.9. Desorption Experiments. The regeneration ability of OMts was investigated by soaking the used adsorbent in ethanol at 25 °C for 1 h. The readsorption experiments were carried out under the same conditions as the adsorption experiments.

3. RESULTS AND DISCUSSION

3.1. Surface Activity. The surface tension of QAS·Y^- as a function of concentration is shown in Figure 2. The critical

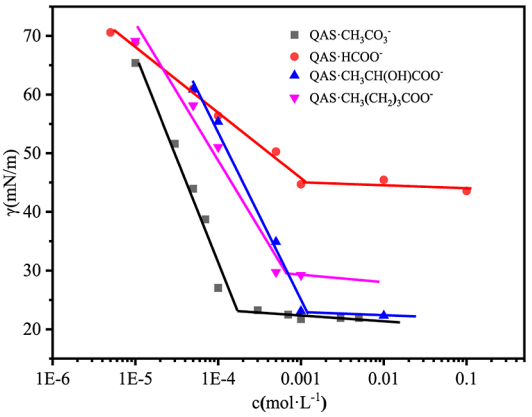

Figure 2. Plots of surface tension (γ) versus the concentration (c) of four surfactants at 298.15 K.

micelle concentration (CMC) and the corresponding minimum surface tension (γ_{CMC}) derived from Figure 2 are listed in Table 1. As seen in Table 1, all four surfactants have excellent surface activity. The CMC values of QAS·$CH_3CO_3^-$, QAS·$CH_3(CH_2)_3COO^-$, QAS·$CH_3CH(OH)COO^-$, and QAS·$HCOO^-$ are 1.56×10^{-4}, 7.22×10^{-4}, 1.12×10^{-3}, and 1.17×10^{-3} mol·L^{-1} at 298.15 K, respectively, and their γ_{CMC} values are between 23.10 and 44.82 mN·m^{-1}.

Table 1. Surface Activity Parameters of Four Surfactants at 298.15 K

compound	CMC (mol·L^{-1})	γ_{CMC} (mN·m^{-1})	pC_{20} (mol·L^{-1})	ΔG_m^θ (KJ·mol^{-1})
QAS·$CH_3CO_3^-$	1.56×10^{-4}	24.02	4.58	−31.67
QAS·$HCOO^-$	1.17×10^{-3}	44.82	3.58	−26.68
QAS·$CH_3CH(OH)COO^-$	1.12×10^{-3}	23.10	4.13	−26.78
QAS·$CH_3(CH_2)_3COO^-$	7.22×10^{-4}	29.42	3.95	−27.87

https://doi.org/10.1021/acsomega.4c08924
ACS Omega 2025, 10, 10926−10937

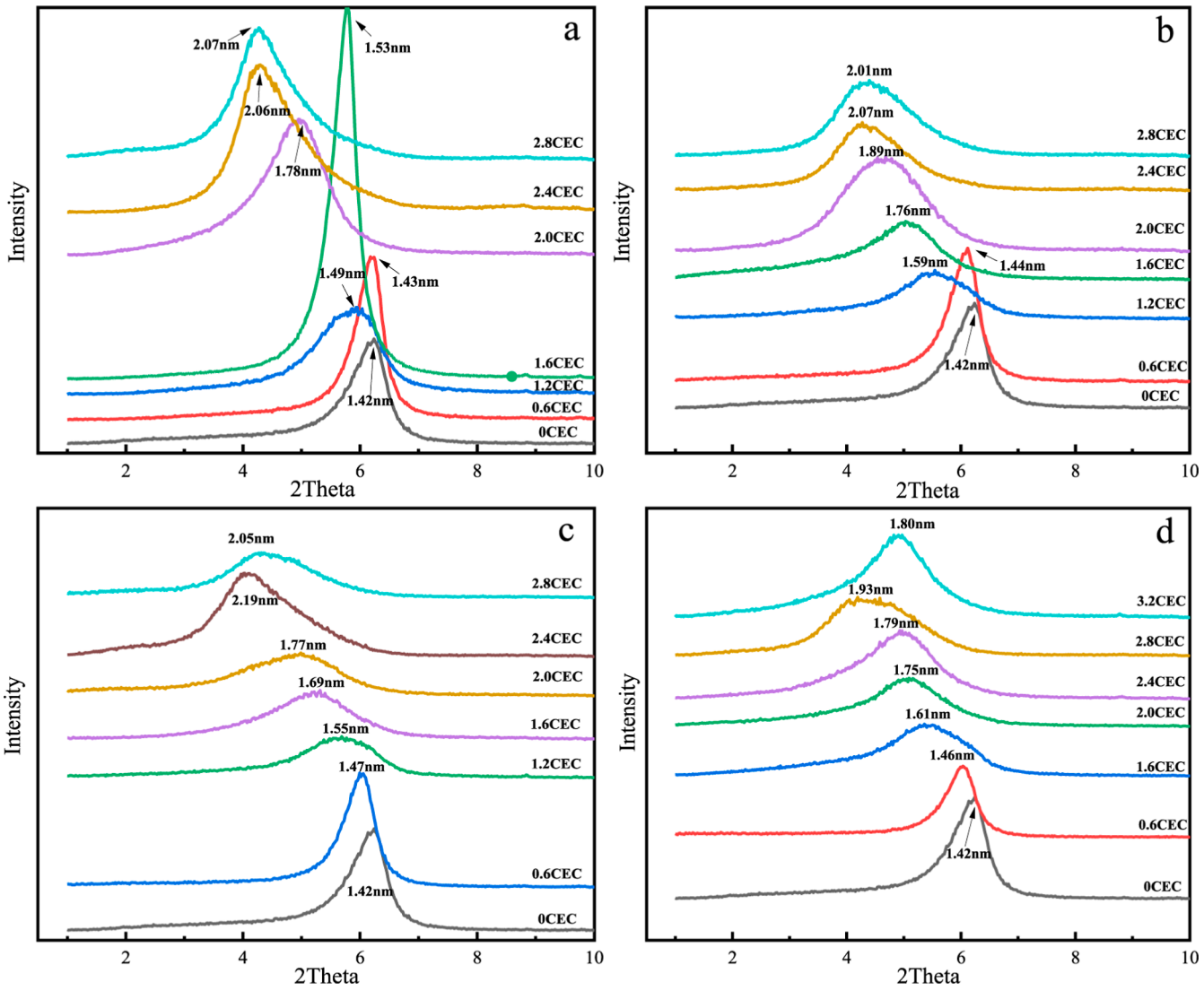

Figure 3. XRD patterns of Na-Mt, OMt-QAS·$CH_3CO_3^-$ (a), OMt-QAS·$HCOO^-$ (b), OMt-QAS·$CH_3CH(OH)COO^-$ (c), and OMt-QAS·$CH_3(CH_2)_3COO^-$ (d).

The pC_{20}, the negative logarithm of the surfactant molarity required to reduce the surface tension of the solvent by 20 $mN{\cdot}m^{-1}$, is a measure of surfactant efficiency. The standard Gibbs free energy of micellization (ΔG_m^θ) is calculated according to Rosen's methodology[32]

$$\Delta G_m^\Theta = RT\ln\left(\frac{CMC}{55.5}\right) \tag{10}$$

These pC_{20} and ΔG_m^θ values are also listed in Table 1. The order of pC_{20} for the four surfactants are QAS·$CH_3CO_3^-$ > QAS·$CH_3CH(OH)COO^-$ > QAS·CH_3 $(CH_2)_3COO^-$ > QAS·$HCOO^-$, indicating that QAS·$CH_3CO_3^-$ is the most efficient in reducing the surface tension. The ΔG_m^θ values of all the four surfactants are negative, indicating that the micellization are spontaneous process at 298.15 K. Furthermore, the absolute ΔG_m^θ values of QAS·$CH_3CO_3^-$, QAS·$CH_3(CH_2)_3COO^-$, QAS·$CH_3CH(OH)COO^-$, and QAS·$HCOO^-$ decrease in a consecutive order, suggesting that the formation and aggregation of micelles are becoming increasingly unfavorable.

3.2. X-ray Diffraction Analysis. The XRD spectra of Na-Mt and OMts modified under 0.6 to 3.2 CEC modification conditions are shown in Figure 3. As shown in Figure 3, the original Na-Mt produces a strong d_{001} plane diffraction peak at $2\theta = 6.22°$. In comparison with Na-Mt, the diffraction peaks of OMts are all shifted to a smaller angle, indicating that all four quaternary ammonium surfactants are successfully inserted into the inner space of Na-Mt. According to the Bragg formula, the interlayer spacing of these OMts has been expanded accordingly. Meanwhile, the interlayer spacing increases gradually as the amount of QAS·$CH_3CO_3^-$, QAS·$HCOO^-$, and QAS·CH_3 $CH(OH)COO^-$ increases from 0.6 to 2.4 CEC, whereas the interlayer spacing basically remains unchanged or even decreases slightly with their amount increasing from 2.4 to 2.8 CEC. It can be concluded that the steric effect of QAS·$CH_3CO_3^-$, QAS·$HCOO^-$, and QAS·$CH_3CH(OH)COO^-$ has taken into effect and their saturation content in Na-Mt is 2.4 CEC.[33] Similarly, the saturation content of QAS·$CH_3(CH_2)_3COO^-$ in Na-Mt is 2.8 CEC.

In addition, Figure 3 shows that the order of the interlayer spacing is as follows: OMt-QAS·$CH_3CH(OH)COO^-$ > OMt-QAS·$HCOO^-$ > OMt-QAS·$CH_3CO_3^-$ > OMt-QAS·$CH_3(CH_2)_3COO^-$, when the amount of modifier QAS·Y^- inserted between the Mt layers is saturated. One of the reasons may be that, compared with QAS·$CH_3CH(OH)$ COO^- and

https://doi.org/10.1021/acsomega.4c08924
ACS Omega 2025, 10, 10926−10937

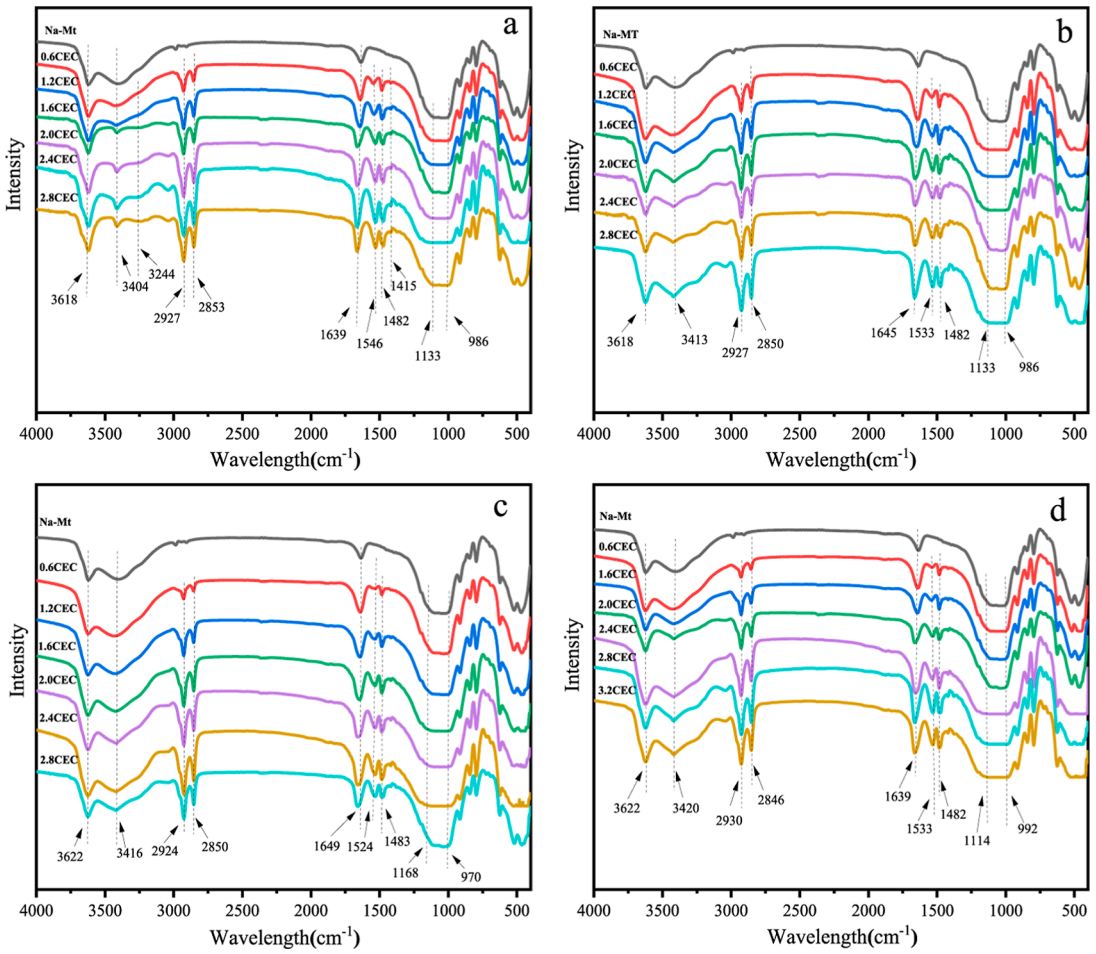

Figure 4. FTIR spectra of Na-Mt, OMt-QAS·$CH_3CO_3^-$ (a), OMt-QAS·$HCOO^-$ (b), OMt-QAS·$CH_3CH(OH)COO^-$ (c), and OMt-QAS·$CH_3(CH_2)_3COO^-$ (d).

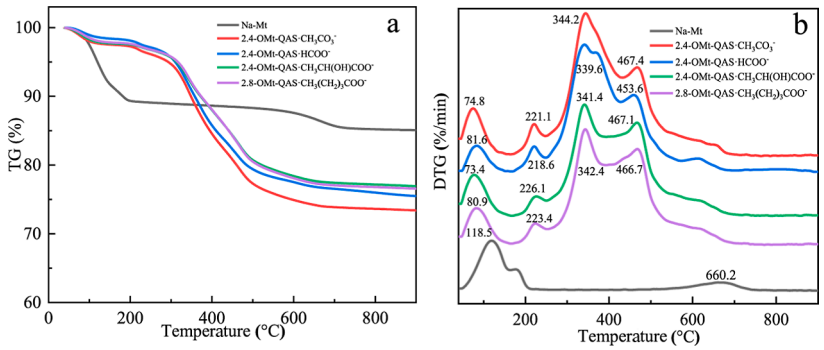

Figure 5. TG (a) and DTG (b) curves of Na-Mt and OMts.

QAS·$HCOO^-$, QAS·$CH_3CO_3^-$ and QAS·$CH_3(CH_2)_3COO^-$ have lower CMCs and are more prone to form micelles; thus, there are fewer free surfactant monomer molecules in solution, thus hindering the ion exchange between the Mt layers. Furthermore, we speculate that the interlayer spacing of OMt may also be influenced by the affinity of the counterions to the long aliphatic chains. $CH_3CO_3^-$, $CH_3CH(OH)C\ OO^-$, and $HCOO^-$ have a weak affinity with aliphatic chains and cannot shield electrostatic repulsion between ion heads, resulting in a looser interlayer arrangement and larger interlayer spacing. Conversely, $CH_3(CH_2)_3COO^-$ is more hydrophobic and has a strong affinity with aliphatic long chains, which results in a more compact arrangement of the hydrophobic long chains of surfactants and a smaller interlayer spacing.[34]

3.3. FTIR Analysis. The FTIR spectra of Na-Mt and OMts under different CEC modification conditions are given in Figure 4. The sharp absorption band of Na-Mt at 3618 cm^{-1} is attributed to the stretching vibration of −OH groups between Mt layers, whereas the peaks at 3404 and 1639 cm^{-1} belong to the stretching vibration peak and bending vibration peak of H−O−H.[35] Meanwhile, the peaks at 1133 and 986 cm^{-1} are attributed to the out of plane and in-plane stretching vibration of Si−O bond, and the bands in the range of 600−400 cm^{-1} correspond to the bending vibration peaks of Si−O−Si and Al−O−Si.[36]

https://doi.org/10.1021/acsomega.4c08924
ACS Omega 2025, 10, 10926−10937

As shown in Figure 4a, the FTIR spectra of OMt-QAS·$CH_3CO_3^-$ under different CEC modification conditions exhibit not only the characteristic absorption bands of Na-Mt but also some characteristic absorption bands of QAS·$CH_3CO_3^-$. Among them, the band at 3244 cm^{-1} is attributed to the stretching vibration of the N−H bond, while the bands at 2927 and 2853 cm^{-1} are attributed to the stretching vibration of the C−H bond of $-CH_3$ and $-CH_2-$. The bands at 1546 and 1482 cm^{-1} correspond to the bending vibration of N−H and the bending vibration of the C−H bond of $-CH_3$, respectively. The peak at 1415 cm^{-1} is due to the stretching vibration of CO_3^- in $CH_3CO_3^-$.

For the other three OMts (Figure 4b−d), the chemical absorption peak of C−O bond of $HCOO^-$ and−OH bond of $CH_3CH(OH)COO^-$ coincide with that of Na-Mt. Furthermore, the chemical absorption peak of $-CH_3$ and $-CH_2-$ bond of $CH_3(CH_2)_3COO^-$ also coincide with that of the cationic fragment of QAS·$CH_3(CH_2)_3COO^-$. Consequently, their FTIR spectrum displays only the characteristic absorption peaks of Na-Mt and the cationic fragment of QAS·Y^-, as do the FTIR spectra of OMt-QAS·$CH_3CO_3^-$, and are not listed individually. The results demonstrate that all four surfactants QAS·Y^- have been successfully incorporated into the interlayer or adsorbed on the surface of Na-Mt.

3.4. TG-DTG Analysis. The thermogravimetric (TG) spectrum (Figure 5a) shows that when the temperature is lower than 200 °C, the mass loss of 2.4-OMt-QAS·$CH_3CO_3^-$ (2.74%), 2.4-OMt-QAS·$HCOO^-$ (1.90%), 2.4-OMt-QAS·$CH_3CH(OH)COO^-$ (2.47%), and 2.8-OMt-QAS·$CH_3(CH_2)_3COO^-$ (2.36%) is less than that of Na-Mt (10.67%), which indicates that there is less free water in OMts. It is due to the fact that the insertion of the surfactant QAS·Y^- into the Mt layers or its adsorption on the surface will reduce the surface energy of Mt, and the hydrophilic surface becomes more hydrophobic.[37] Above 200 °C, Na-Mt has less mass loss (4.26%) compared with 2.4-OMt-QAS·$CH_3CO_3^-$ (23.85%), 2.4-OMt-QAS·$HCOO^-$ (22.62%), 2.4-OMt-QAS·$CH_3CH(OH)COO^-$ (20.60%), and 2.8-OMt-QAS·$CH_3(CH_2)_3COO^-$ (21.07%), which is due to the thermal decomposition of the surfactant QAS·Y^- in this process. It also shows that the thermal stability of OMt is worse than that of Na-Mt.[38]

From the derivative thermogravimetric (DTG) curve (Figure 5b), it can be seen that all samples, including Na-Mt and the four OMts, exhibit a peak at temperatures below 200 °C. This phenomenon is attributed to the detachment of free and physiosorbed water between layers and on the surface of Mt. The peak observed at 660.2 °C in Na-Mt can be attributed to the dihydroxylation of the −OH group situated between the Mt layers.[39,40] The four OMts all have three peaks between 200 and 600 °C, while Na-Mt does not. Therefore, the mass loss within this temperature range is attributed to the thermal decomposition of surfactant QAS·Y^-.

3.5. N_2 Adsorption/Desorption Isotherms. The N_2 adsorption/desorption isotherms of Na-Mt and OMts are shown in Figure 6. According to the classification of IUPAC, their adsorption isotherms are Type IV isotherms with H3 hysteresis loop.[41] The adsorption curve is inconsistent with the analytical curve and does not show adsorption saturation under relatively high relative pressure, indicating that Mt is a mesoporous material.[42] Specific surface area (S_{BET}), total pore volume (V_t), and average pore radius (D_p) of Na-Mt and OMts are shown in Table 2. Note that, S_{BET} and V_t of the four

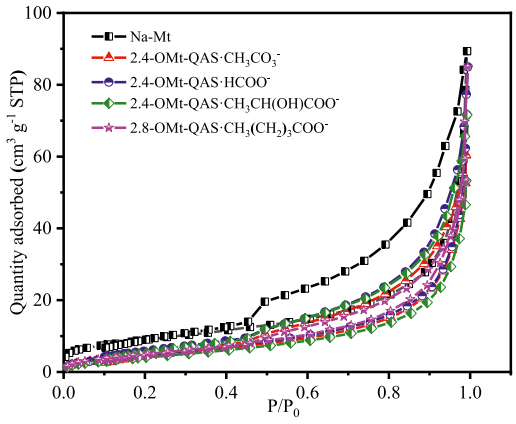

Figure 6. Nitrogen adsorption−desorption isotherms of Na-Mt and OMts.

Table 2. Porous Structural Data of Na-Mt and OMts

sample	S_{BET}[a] (m^2/g)	V_t[b] (m^3/g)	D_p[c] (nm)
Na-Mt	32.514	0.138	16.978
2.4-OMt-QAS·$CH_3CO_3^-$	18.437	0.094	20.286
2.4-OMt-QAS·$HCOO^-$	19.607	0.131	26.826
2.4-OMt-QAS·$CH_3CH(OH)COO^-$	19.191	0.111	23.093
2.8-OMt-QAS·$CH_3(CH_2)_3COO^-$	16.330	0.082	20.174

OMts are all smaller than that of Na-Mt, but D_p is slightly increased. The decrease of S_{BET} and V_t may be due to the fact that the surfactant QAS·Y^- is inserted between Mt layers or organic chains are grafted on the surface of Mt, blocking part of the structural channels, thus restricting the entry of N_2.[43]

3.6. Adsorption of 2,4-Dichlorophenol/Cibacron Brilliant Yellow 3G-P on OMts. *3.6.1. Effect of Surfactant Addition.* Figure 7 shows the trend of adsorption of 2,4-dichlorophenol/cibacron brilliant yellow 3G-P by four OMts under different modifier dosage. It can be found that for OMt-QAS·$CH_3CO_3^-$, OMt-QAS·$HCOO^-$, and OMt-QAS·$CH_3CH(OH)COO^-$, their adsorption capacity for 2,4-dichlorophenol/cibacron brilliant yellow 3G-P gradually increases with the amount of modifier increases from 0 to 2.4 CEC. It was because the interlayer spacing of Mt gradually increases with the increase of modifier, thus improving its adsorption capacity. Second, the amphiphilic nature of surfactants endows the surface and interlayer of OMts with the hydrophobic groups of the surfactant, thereby greatly increasing the hydrophobicity of Mt and thus improving the adsorption capacity of organic pollutants.[44] As the amount of the modifier increases from 2.4 to 3.0 CEC, the adsorption capacity of the three OMts for 2,4-dichlorophenol/cibacron brilliant yellow 3G-P remains unchanged or even decreases. This may be due to the accumulation of the additional surfactant molecules between Mt chips, occupying the active sites and interlayer space originally used for 2,4-dichlorophenol/cibacron brilliant yellow 3G-P adsorption, thus reducing the adsorption capacity.[23] Similarly, OMt-QAS·$CH_3(CH_2)_3COO^-$ modified under 2.8 CEC has the best adsorption capacity.

3.6.2. Effect of Adsorbent Dosage. Figure 8 exhibits the adsorption effects of OMts on organic pollutants at different dosages. The adsorption capacity of all four OMts for 2,4-dichlorophenol/cibacron brilliant yellow 3G-P decreases gradually with the increase of OMts addition. This is due to the fact that the more OMt is added, the less OMt is bound to

https://doi.org/10.1021/acsomega.4c08924
ACS Omega 2025, 10, 10926−10937

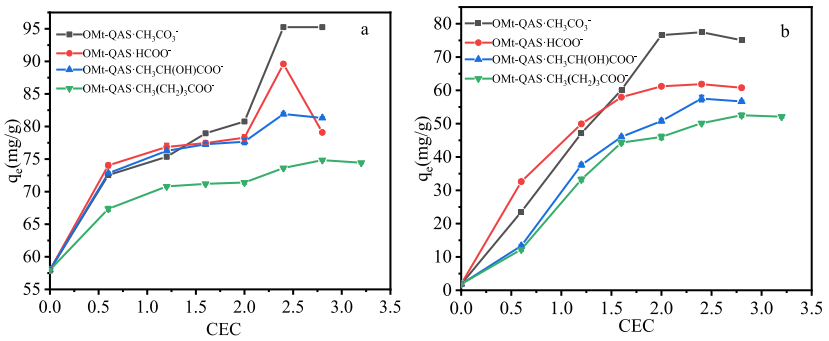

Figure 7. Effect of modifier dosage on the adsorption of 2, 4-dichlorophenol (a) and cibacron brilliant yellow 3G-P (b) by OMts.

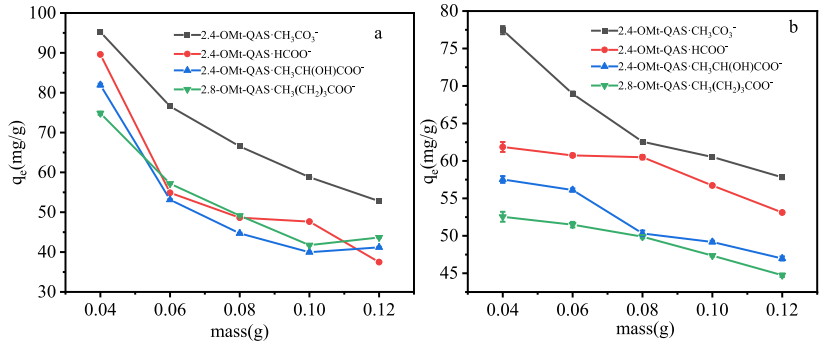

Figure 8. Effect of OMts addition on 2, 4-dichlorophenol (a) and cibacron brilliant yellow 3G-P (b) adsorption.

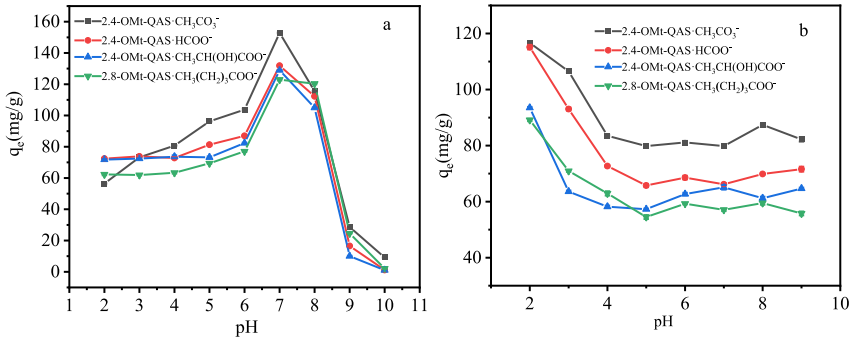

Figure 9. Effect of pH on the adsorption of 2, 4-dichlorophenol (a) and cibacron brilliant yellow 3G-P (b) by OMts.

2,4-dichlorophenol/cibacron brilliant yellow 3G-P molecules per unit area, and thus there are abundant vacant adsorbent sites on OMt, reducing the adsorption efficiency of OMt. Second, at the current concentration and volume of 2, 4-dichlorophenol/cibacron brilliant yellow 3G-P solution, an increase in the amount of OMt dosage and solid−liquid ratio results in an elevated viscosity of the system and a concomitant reduction in the dispersion of OMt.[45] Consequently, a proportion of OMt is unable to fully utilize its own adsorption capacity. It may also be that the aqueous solution of the adsorbent is acidic, and excessive addition will reduce the pH of the system, which may have a certain impact on the adsorption effect of 2, 4-dichlorophenol.

3.6.3. Effect of pH. The adsorption effects of OMts on 2, 4-dichlorophenol/cibacron brilliant yellow 3G-P at different pH are presented in Figure 9. From Figure 9a, it can be seen that the adsorption capacity of the four OMts on 2, 4-dichlorophenol first increases and then decreases as the pH of the system increases from 2 to 10, and the best adsorption effect is observed at pH 7. The surface charge of OMt and the form of 2, 4-dichloropheno present at different pH are responsible for this phenomenon.[46] It is known that the pK_a of 2, 4-dichlorophenol is 7.89, So, at pH 2−7, 2, 4-dichlorophenol presents in an uncharged molecular form in the solution.[44] The ion dipole interaction between the hydroxyl group of 2, 4-dichlorophenol and the cationic headgroup of quaternary ammonium surfactant QAS·Y^- is conducive to the adsorption of 2, 4-dichlorophenol. In addition, neutral 2, 4-dichlorophenol molecules are more adsorbed on organic clay compared to anionic molecules because the organic phase acts as an effective distribution medium for the uptake of neutral 2, 4-dichlorophenol at low pH or acidic conditions.[47] Above pH 7, the 2, 4-dichlorophenol molecules are in negative charge. Meanwhile, the surface of the three OMts is also negatively charged above pH 7 since the PZC of 2.4-OMt-QAS·$HCOO^-$, 2.4-OMt-QAS·$CH_3CH(OH)COO^-$, and 2.8-OMt-QAS·$CH_3(CH_2)_3COO^-$ is 6.02, 5.45, and 6.87, respectively (Figure 10). The electrostatic repulsion between negatively charged OMts and negatively charged 2, 4-dichlorophenol is not favorable for adsorption. In addition, as presented in Figure 10,

https://doi.org/10.1021/acsomega.4c08924
ACS Omega 2025, 10, 10926−10937

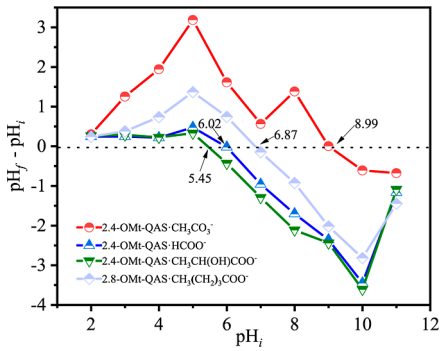

Figure 10. PZC of OMts.

the PZC of 2.4-OMt-QAS·$CH_3CO_3^-$ is 8.99. When pK_a < pH < 8.99, 2, 4-dichlorophenol is negatively charged, and the surface of 2.4-OMt-QAS·$CH_3CO_3^-$ is negatively charged and the edges charged, which is conducive to the adsorption of 2, 4-dichlorophenol on the whole surface of Mt. This may be one of the reasons for the relatively better adsorption of 2.4-OMt-QAS·$CH_3CO_3^-$ under the same pH condition.

In addition, As shown in Figure 9b, the adsorption capacity of the four OMts on cibacron brilliant yellow 3G-P decreases when the pH of the system increases from 2 to 5, while their adsorption capacities do not change significantly when the pH value increases from 5 to 9, and the best adsorption effect is observed at pH 2. When 2 < pH < 5, the cibacron brilliant yellow 3G-P molecules are in the negative charge and the surface of the OMts is positively charged, so it is favorable for the adsorption of activated yellow, and the smaller the pH is, the more favorable the adsorption is. As the system pH increases from 6 to 9, the negative charge on the surface of the OMts increases, which is unfavorable for adsorption. Also, in alkaline medium, there will be competition between the OH^- ions and the anions of cibacron brilliant yellow 3G-P.[48] Thus, all four OMts maintain a relatively stable but much smaller adsorption capacity than that at pH 2.

Figure 9 also shows that the maximum adsorption capacities of 2.4-OMt-QAS·$CH_3CO_3^-$, 2.4-OMt-QAS·$HCOO^-$, 2.4-OMt-QAS·$CH_3CH(OH)$ CO O^-, and 2.8-OMt-QAS·$CH_3(CH_2)_3COO^-$ for 2, 4-dichlorophenol/cibacron brilliant yellow 3G-P can reach 152.85/116.17, 131.84/115.5, 131.03/93.49, and 122.94/89.15 mg/g, respectively. In comparison with the initial capacity of Na-Mt, which is 58/1.85 mg/g, the adsorption effect was greatly improved. Moreover, under the same initial concentration of the 2, 4-dichlorophenol/cibacron brilliant yellow 3G-P solution, the adsorption capacity of the four OMts is also better than that of some organic modified clay or other types of adsorbent given in the literature.[49−53] In addition, it can be seen that the order of the maximum adsorption capacities of the four OMts for 2, 4-dichlorophenol/cibacron brilliant yellow 3G-P does not coincide with the order of their interlayer spacings. It is postulated that in addition to the interlayer spacing, the PZC of OMt also influences its adsorption properties.

3.7. Adsorption Kinetics. As shown in Figures S1 and S2, with the time, the adsorption of 2, 4-dichlorophenol/cibacron brilliant yellow 3G-P by four OMts increases at 25, 35, and 45 °C, with a rapid increase in the first 100 min and then gradually reaching equilibrium. This phenomenon can be attributed to the presence of a considerable number of adsorption active sites on the interlayer and surface of OMts initially, which gradually become saturated as the contact time increases.

Figure S1 also shows that the adsorption performance of the four OMts for 2, 4-dichlorophenol exhibits a slight decline as the adsorption temperature increases from 25 to 45 °C, indicating that the adsorption process is exothermic. This may be because the arrangement of surfactant alkyl chains within the Mt sheet changes, or the diffusion mass transfer resistance increases as the temperature increases.[54,55] Conversely, as seen from Figure S2, the adsorption performance of the four OMts for cibacron brilliant yellow 3G-P demonstrates a slight increase as the temperature increases, suggesting that the adsorption process is endothermic. This may be due to the fact that the molecular structure of cibacron brilliant yellow 3G-P is larger and more complex than that of 2, 4-dichlorophenol, which makes the adsorption of cibacron bright yellow 3G-P more difficult and requires more energy.

The relevant kinetic parameters, as derived from the kinetic fit curves (Figures S3−S5), are listed in Tables S1 and S2. It can be seen that the q_{ecal} values derived from the pseudo-second-order model are in close agreement with the corresponding experimental values. Furthermore, the R_2^2 values of the pseudo-second-order model exceed the R_1^2 values of the pseudo-first-order model and are very close to 1. Consequently, it can be inferred that the pseudo-second-order mechanism predominantly governs the adsorption of 2, 4-dichlorophenol/cibacron brilliant yellow 3G-P by OMts.

The three linear regions observed in Figure S5 indicate that the adsorption process of 2, 4-dichlorophenol/cibacron brilliant yellow 3G-P on OMts can be divided into three distinct stages. The initial stage is characterized by instantaneous outer surface adsorption, whereby the fitting line displays the greatest steepness and highest slope, indicating a rapid adsorption rate. The second stage is characterized by stepwise adsorption, whereby the diffusion rate of the 2, 4-dichlorophenol/cibacron brilliant yellow 3G-P molecules exerts a dominant influence on the overall adsorption process. The third stage is the equilibrium stage. Due to the lower concentration of adsorbed substances and fewer active adsorption points, the internal diffusion of the particles becomes slower and slower. In addition, as shown in Figure S5, all the obtained lines do not pass through the origin, indicating that the mechanism of the adsorption process does not only follow intraparticle diffusion but also involves other mechanisms such as external liquid film diffusion, distribution, and surface diffusion. Moreover, the correlation coefficients R^2 obtained from the intraparticle diffusion model for the four OMts all are larger than 0.88 (Table S2), indicating that the intraparticle diffusion process plays a significant role in the adsorption of 2, 4-dichlorophenol/cibacron brilliant yellow 3G-P.[4]

3.8. Adsorption Isotherms. Figure S6 shows the adsorption isotherm of 2, 4-dichlorophenol/cibacron brilliant yellow 3G-P onto OMts under equilibrium conditions. From the estimated values of the corresponding parameters (Table S3), it can be seen that the adsorption of 2, 4-dichlorophenol/cibacron brilliant yellow 3G-P by the four OMts is all better modeled by Freundlich isotherm than that by Langmuir isotherms, with the linear correlation coefficients R^2 of the Freundlich model ≥0.9655, indicating that the two pollutants are adsorbed in the four OMts in a multilayer arrangement. In addition, the 1/n values in the Freundlich isotherm model are less than 1 for all samples, suggesting that these adsorption

https://doi.org/10.1021/acsomega.4c08924
ACS Omega 2025, 10, 10926−10937

Table 3. Thermodynamic Parameters of Adsorption of 2, 4-Dichlorophenol by OMts

OMt	C_0	ΔH	ΔS	ΔG (kJ/mol)					R^2
	(mg/L)	(kJ/mol)	(J·mol^{-1}·K^{-1})	298 K	308 K	318 K	328 K	338 K	
2.4-OMt-QAS·$CH_3CO_3^-$	100	−2.62	−5.37	−1.02	−0.97	−0.91	−0.86	0.80	0.988
2.4-OMt-QAS·$HCOO^-$	100	−7.68	−22.80	−0.89	−0.66	−0.43	−0.20	0.03	0.925
2.4-OMt-QAS·$CH_3CH(OH)COO^-$	100	−5.09	−15.59	−0.44	−0.29	−0.13	0.02	0.18	0.983
2.8-OMt-QAS·$CH_3(CH_2)_3COO^-$	100	−2.27	−6.71	−0.27	−0.20	−0.14	−0.07	−0.002	0.976

Table 4. Thermodynamic Parameters of Adsorption of Cibacron Brilliant Yellow 3G-P by OMts

OMt	C_0	ΔH	ΔS	ΔG (kJ/mol)					R^2
	(mg/L)	(kJ/mol)	(J·mol^{-1}·K^{-1})	298 K	308 K	318 K	328 K	338 K	
2.4-OMt-QAS·$CH_3CO_3^-$	100	8.191	28.268	−0.23	−0.52	−0.80	−1.08	−1.36	0.928
2.4-OMt-QAS·$HCOO^-$	100	5.371	16.828	0.36	0.19	0.02	−0.15	−0.32	0.801
2.4-OMt-QAS·$CH_3CH(OH)COO^-$	100	3.746	10.010	0.76	0.66	0.56	0.46	0.36	0.964
2.8-OMt-QAS·$CH_3(CH_2)_3COO^-$	100	4.243	10.974	0.97	0.86	0.75	0.64	0.53	0.947

processes are spontaneous physical processes and favorably nonlinear heterogeneous. It is also found that 2.4-OMt-QAS·$CH_3CO_3^-$ adsorbs 2, 4-dichlorophenol/cibacron brilliant yellow 3G-P with the largest k_F value, indicating the best adsorption capacity.[56]

3.9. Thermodynamic Parameters. These thermodynamic parameters are listed in Tables 3 and 4. At 298, 308, and 318 K, the values of $\Delta G°$ are negative (Table 3), confirming that the adsorption of 2, 4-dichlorophenol onto the four OMts has a natural tendency to proceed spontaneously. At the same time, as shown in Table 3, all ΔG values are greater than −20 kJ/mol, indicating that the adsorption process of 2, 4-dichlorophenol is dominated by physical adsorption.[57] Furthermore, for each OMt, the value of ΔG increases with the increase in temperature, indicating that the increase in temperature is not conducive to the adsorption of the 2, 4-dichlorophenol solution by OMts. In addition, for each OMt, ΔH is also less than 0, which further confirms that the adsorption reaction of 2, 4-dichlorophenol by OMts is exothermic, consistent with the result that the adsorption capacity decreases with an increase of temperature. The values of $\Delta S°$ are negative, indicating a reduction in the randomness at the solid/liquid interface during the adsorption process.[19]

As can be seen from Table 4, for each OMt, the ΔG value decreases with the increase in temperature, indicating that the increase in temperature is favorable for the adsorption of cibacron brilliant yellow 3G-P solution by the four OMts. In addition, all the values of ΔH are positive, which further confirms that the reaction of adsorption cibacron brilliant yellow 3G-P of OMt is endothermic, consistent with the result that the adsorption capacity increases with the increase in temperature.

3.10. Desorption Tests. In order to verify the reusability of the four OMts, the 2.4-OMt-QAS·$CH_3CO_3^-$, 2.4-OMt-QAS·$HCOO^-$, 2.4-OMt-QAS·CH_3CH $(OH)COO^-$, and 2.8-OMt-QAS·$CH_3(CH_2)_3COO^-$ with the best adsorption performance described above are used to conduct the desorption and adsorption experiments of 2, 4-dichlorophenol. The results are shown in Figure 11. It can be found that the four OMts still have 60−70% adsorption capacity after five adsorption desorption cycles, indicating that they have a certain renewable capacity through ethanol washing. Moreover, through further distillation, 2, 4-dichlorophenol and anhydrous ethanol can be easily recovered. The difference in adsorption capacity between continuous cycles may be caused by the stubborn interaction between the adsorbent OMts and 2, 4-dichlorophenol.[58]

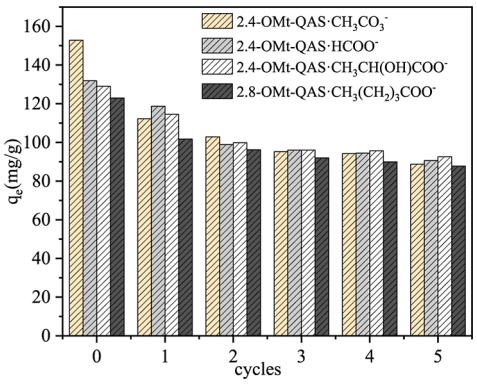

Figure 11. Reusability of OMts for 2, 4-dichlorophenol adsorption.

4. CONCLUSIONS

In this study, 2, 4-dichlorophenol/cibacron brilliant yellow 3G-P is removed from aqueous solution using OMts modified by quaternary ammonium surfactants containing different organic counterions. When their initial concentration is 100 mg/L, by optimizing the adsorption conditions, the maximum adsorption capacities of 2.4-OMt-QAS·$CH_3CO_3^-$, 2.4-OMt-QAS·$HCOO^-$, 2.4-OMt-QAS·$CH_3CH(OH)COO^-$, and 2.8-OMt-QAS·$CH_3(CH_2)_3COO^-$ for 2, 4-dichlorophenol/cibacron brilliant yellow 3G-P can reach 152.85/116.17, 131.84/115.5, 131.03/93.49, and 122.94/89.15 mg/g, respectively. The adsorption effect has been greatly improved compared to the initial capacity of Na-Mt of 58/1.85 mg/g. The kinetic studies indicate that all adsorption processes follow the pseudo-second-order model, and the intraparticle diffusion model also plays a significant role. The equilibrium data of the four OMts fit well to the Freundlich model. The thermodynamic parameters indicate that the adsorption of 2, 4-dichlorophenol is a physical, spontaneous, and exothermic process, while the adsorption of cibacron brilliant yellow 3G-P is a physical, spontaneous, and endothermic process. In addition, after five adsorption desorption cycles through ethanol washing, the four OMts still have 60−70% adsorption capacity for 2, 4-dichlorophenol.

It is worth noting that the structure and hydrophobicity of the counterions as well as the affinity of the counterions with

https://doi.org/10.1021/acsomega.4c08924
ACS Omega 2025, 10, 10926−10937

the long aliphatic chains influence the interlayer spacing of OMt. The counterion with stronger hydrophilicity and weaker affinity for aliphatic chains is beneficial to the expansion of the interlayer spacing of OMt. In addition, it is speculated that the counterions also have an effect on the PZC of OMts, thereby affecting the adsorption properties of OMts. This study is important for designing Mt-based organoclay adsorbents for the removal of organic pollutants from industrial wastewater.

■ ASSOCIATED CONTENT

Supporting Information

The Supporting Information is available free of charge at https://pubs.acs.org/doi/10.1021/acsomega.4c08924.

Synthesis route of QAS·Y^-; effect of contact time and temperature on the adsorption properties of OMts; kinetic model of the adsorption; isotherms model of the adsorption; kinetics parameters; and isotherm constants (PDF)

■ AUTHOR INFORMATION

Corresponding Author

Hongqin Liu − *China Food Flavor and Nutrition Health Innovation Center, Beijing Technology and Business University, Beijing 100048, China;* orcid.org/0000-0003-2051-0342; Email: liuhongqin@th.btbu.edu.cn

Authors

Runyu Cao − *China Food Flavor and Nutrition Health Innovation Center, Beijing Technology and Business University, Beijing 100048, China*

Bowen Guan − *China Food Flavor and Nutrition Health Innovation Center, Beijing Technology and Business University, Beijing 100048, China*

Siqi Hu − *Institute of Traditional Chinese Medicine Health Industry, China Academy of Chinese Medical Sciences, Nanchang 330038, China*

Xinru Jia − *China Food Flavor and Nutrition Health Innovation Center, Beijing Technology and Business University, Beijing 100048, China*

Baocai Xu − *China Food Flavor and Nutrition Health Innovation Center, Beijing Technology and Business University, Beijing 100048, China*

Complete contact information is available at: https://pubs.acs.org/10.1021/acsomega.4c08924

Notes

The authors declare no competing financial interest.

■ ACKNOWLEDGMENTS

This study was supported by the National Key R&D Program of China (2017YFB0308701) and the Fundamental Research Funds for the Central Public Welfare Research Institutes (ZZ16-ND-12).

■ REFERENCES

(1) Isa, M. H.; Wong, L. P.; Mubarak, N. M. Editorial: Advances in removal of toxic substances from wastewater. *Front. Environ. Sci.* **2023**, *11*, 1165882.

(2) Hamidon, T. S.; Adnan, R.; Haafiz, M. K. M.; Hussin, M. H. Cationic surfactant-modified cellulose nanocrystal/alginate hydrogel beads for enhanced adsorptive removal of 4-chlorophenol from wastewater. *J. Polym. Environ.* **2022**, *30*, 5024−5048.

(3) Yang, Q.; Gao, M.; Zang, W. Comparative study of 2,4,6-trichlorophenol adsorption by montmorillonites functionalized with surfactants differing in the number of head group and alkyl chain. *Colloids Surf. A Physicochem. Eng. Asp.* **2017**, *520*, 805−816.

(4) Liu, S.; Huang, B.; Zheng, G.; Zhang, P.; Li, J.; Yang, B.; Chen, Y.; Liang, L. Nanocapsulation of horseradish peroxidase (HRP) enhances enzymatic performance in removing phenolic compounds. *Int. J. Biol. Macromol.* **2020**, *150*, 814−822.

(5) Wang, B.; Huang, Q.; Venkitasamy, C.; Chai, H.; Gao, H.; Cheng, N.; Cao, W.; Lv, X.; Pan, Z. Changes in phenolic compounds and their antioxidant capacities in jujube (Ziziphus jujuba Miller) during three edible maturity stages. *LWT-Food Sci. Technol.* **2016**, *66*, 56−62.

(6) Ghochlavi, N.; Aghapour, A. A.; Khorsandi, H. Biodegradation of 2−4-6 trichlorophenol by sequencing batch reactors (SBR) equipped with a rotating biological bed and operated in an anaerobic-aerobic condition. *Front. Environ. Sci.* **2022**, *10*, 1015790.

(7) Khan, M. A.; Mutahir, S.; Wang, F.; Zhen, H.; Lei, W.; Xia, M.; Ouyang, Y.; Muhmood, T. Synthesis of environmentally encouraged, highly robust pollutants reduction 3-D system consisting of Ag/g-C_3N_4 and Cu-complex to degrade refractory pollutants. *J. Photochem. Photobiol., A* **2018**, *364*, 826−836.

(8) Yasin, M.; Saeed, M.; Muneer, M.; Usman, M.; ul Haq, A.; Sadia, M.; Altaf, M. Development of Bi_2O_3-ZnO heterostructure for enhanced photodegradation of rhodamine B and reactive yellow dyes. *Surf. Interfaces* **2022**, *30*, 101846.

(9) Karimi-Maleh, H.; Ranjbari, S.; Tanhaei, B.; Ayati, A.; Orooji, Y.; Alizadeh, M.; Karimi, F.; Salmanpour, S.; Rouhi, J.; Sillanpää, M.; et al. Novel 1-butyl-3-methylimidazolium bromide impregnated chitosan hydrogel beads nanostructure as an efficient nanobio-adsorbent for cationic dye removal: Kinetic study. *Environ. Res.* **2021**, *195*, 110809.

(10) Mehdizadeh, P.; Orooji, Y.; Amiri, O.; Salavati-Niasari, M.; Moayedi, H. Green synthesis using cherry and orange juice and characterization of $TbFeO_3$ ceramic nanostructures and their application as photocatalysts under UV light for removal of organic dyes in water. *J. Clean. Prod.* **2020**, *252*, 119765.

(11) Alharbi, H. A.; Hameed, B. H.; Alotaibi, K. D.; Al-Oud, S. S.; Al-Modaihsh, A. S. Recent methods in the production of activated carbon from date palm residues for the adsorption of textile dyes: A review. *Front. Environ. Sci.* **2022**, *10*, 103441.

(12) Puchana-Rosero, M. J.; Lima, E. C.; Ortiz-Monsalve, S.; Mella, B.; da Costa, D.; Poll, E.; Gutterres, M. Fungal biomass as biosorbent for the removal of Acid Blue 161 dye in aqueous solution. *Environ. Sci. Pollut. Res.* **2017**, *24*, 4200−4209.

(13) Neetha, J. N.; Ujwal, P.; Sandesh, K.; Santhosh, H.; Girish, K. Aerobic biodegradation of Acid Blue-9 dye by Bacillus fermus Isolated from Annona reticulata. *Environ. Technol. Innov.* **2018**, *11*, 253−261.

(14) Malvar, J. L.; Martín, J.; Orta, M. D. M.; Medina-Carrasco, S.; Alonso, E. Simultaneous and individual adsorption of ibuprofen metabolites by a modified montmorillonite. *Appl. Clay Sci.* **2020**, *189*, 105529.

(15) Peng, H.; Shen, Y.; Luo, M.; Zheng, X.; Wen, J. Polypyrrole-decorated Mg-Al layered double oxides for dye adsorption: Isotherm, kinetics, and thermodynamic investigations. *Chem. Phys. Lett.* **2023**, *824*, 140568.

(16) Zazou, H.; Afanga, H.; Akhouairi, S.; Ouchtak, H.; Addi, A. A.; Akbour, R. A.; Assabbane, A.; Douch, J.; Elmchaouri, A.; Duplay, J.; et al. Treatment of textile industry wastewater by electrocoagulation coupled with electrochemical advanced oxidation process. *J. Water Process Eng.* **2019**, *28*, 214−221.

(17) Yu, F.; Bai, X.; Liang, M.; Ma, J. Recent progress on metal-organic framework-derived porous carbon and its composite for pollutant adsorption from liquid phase. *Chem. Eng. J.* **2021**, *405*, 126960.

(18) Awad, A. M.; Shaikh, S. M. R.; Jalab, R.; Gulied, M. H.; Nasser, M. S.; Benamor, A.; Adham, S. Adsorption of organic pollutants by natural and modified clays: A comprehensive review. *Sep. Purif. Technol.* **2019**, *228*, 115719.

(19) Haounati, R.; Ouachtak, H.; E Haouti, R.; Akhouairi, S.; Largo, F.; Akbal, F.; Benlhachemi, A.; Jada, A.; Addi, A. A. Elaboration and properties of a new SDS/CTAB @Montmorillonite organoclay compositeas a superb adsorbent for the removal of malachite green from aqueous solutions. *Sep. Purif. Technol.* **2021**, *255*, 117335.
(20) Ewis, D.; Ba-Abbad, M.; Benamor, A.; El-Naas, M. Adsorption of organic water pollutants by clays and clay minerals composites: A comprehensive review. *Appl. Clay Sci.* **2022**, *229*, 106686.
(21) Peng, S.; Mao, T.; Zheng, C.; Wu, X.; Wei, Y.; Zeng, Z.; Xiao, R.; Sun, Y. Polyhydroxyl gemini surfactant-modified montmorillonite for efficient removal of methyl orange. *Colloids Surf. A Physicochem. Eng. Asp.* **2019**, *578*, 123602.
(22) Mao, J.; Zhou, Y.; Lv, G.; Zhou, R. Simultaneous detoxification of aflatoxin B1, zearalenone and deoxynivalenol by modified montmorillonites. *Molecules* **2022**, *27*, 315.
(23) Cao, G.; Gao, M.; Shen, T.; Zhao, B.; Zeng, H. Comparison between asymmetric and symmetric gemini surfactant-modified novel organo-vermiculites for removal of phenols. *Ind. Eng. Chem. Res.* **2019**, *58*, 12927−12938.
(24) Tangaraj, V.; Janot, J. M.; Jaber, M.; Bechelany, M.; Balme, S. Adsorption and photophysical properties of fluorescent dyes over montmorillonite and saponite modified by surfactant. *Chemosphere* **2017**, *184*, 1355−1361.
(25) Luo, W.; Huang, Q.; Zeng, P.; Cheng, C.; Yuan, X.; Xiao, T.; Zhang, M.; Antwi, P.; Xing, J.; Ren, S. Gemini surfactant-modified montmorillonite with tetrachloroferrate ($FeCl_4^-$) as a counterion simultaneously sequesters nitrate and phosphate from aqueous solution. *J. Hazard. Mater.* **2021**, *409*, 124829.
(26) Manet, S.; Karpichev, Y.; Bassani, D.; Kiagus-Ahmad, R.; Oda, R. Counter anion effect on micellization of cationic gemini surfactants 14−2-14: hofmeister and other counterions. *Langmuir* **2010**, *26*, 10645−10656.
(27) Shen, T.; Gao, M. Gemini surfactant modified organo-clays for removal of organic pollutants from water: A review. *Chem. Eng. J.* **2019**, *375*, 121910.
(28) Liu, H.; Zhou, X.; Zhang, X.; Shi, G.; Hu, J.; Liu, C.; Xu, B. Green synthesis, surface activity, micellar aggregation, and corrosion inhibition properties of new gemini quaternary ammonium surfactants. *J. Chem. Eng. Data* **2018**, *63*, 1304−1315.
(29) Jia, X.; Wei, R.; Xu, B.; Liu, H.; Xu, B. Green synthesis, surface activity, micellar aggregation, and foam properties of amide quaternary ammonium surfactants. *ACS Omega* **2022**, *7*, 48240−48249.
(30) Ho, Y. S.; McKay, G. Sorption of dye from aqueous solution by peat. *Chem. Eng. J.* **1998**, *70*, 115−124.
(31) Ho, Y. S.; Porter, J. F.; Mckay, G. Equilibrium isotherm studies for the sorption of divalent metal ions onto peat: copper, nickel and lead single component systems. *Water Air Soil Pollut.* **2002**, *141*, 1−33.
(32) Rosen, M. J.; Kunjappu, T. J. *Surfactants and Interfacial Phenomena*, 4 ed.; Wiley: New York, 2012; . th ed.
(33) Li, P.; Khan, M. A.; Xia, M.; Lei, W.; Zhu, S.; Wang, F. Efficient preparation and molecular dynamic (MD) simulations of Gemini surfactant modified layered montmorillonite to potentially remove emerging organic contaminants from wastewater. *Ceram. Int.* **2019**, *45*, 10782−10791.
(34) Willott, J. D.; Murdoch, T. J.; Humphreys, B. A.; Edmondson, S.; Wanless, E. J.; Webber, G. B. Anion-specific effects on the behavior of pH-sensitive polybasic brushes. *Langmuir* **2015**, *31*, 3707−3717.
(35) Bartolozzi, A.; Bertani, R.; Burigo, E.; Fabrizi, A.; Panozzo, F.; Quaresimin, M.; Simionato, F.; Sgarbossa, P.; Tamburini, S.; Zappalorto, M.; Zorzi, F. Multifunctional Cu^{2+}-montmorillonite/epoxy resin nanocomposites with antibacterial activity. *J. Appl. Polym. Sci.* **2017**, *134*, 44733.
(36) Al-Mosawy, A. A.; Al-Mulla, E. A. J. Preparation of new nano-organoclays from hexadecylamine, tetradecylamine and chalcone with montmorillonite using ion exchange processes. *Epitoanyag* **2018**, *70*, 116−119.
(37) Martins, M. G.; Martins, D. O. T. A.; de Carvalho, B. L. C.; Mercante, L. A.; Soriano, S.; Andruh, M.; Vieira, M. D.; Vaz, M. G. F. Synthesis and characterization of montmorillonite clay intercalated with molecular magnetic compounds. *J. Solid State Chem.* **2015**, *228*, 99−104.
(38) Yang, Q.; Gao, M.; Luo, Z.; Yang, S. Enhanced removal of bisphenol A from aqueous solution by organo-montmorillonites modified with novel Gemini pyridinium surfactants containing long alkyl chain. *Chem. Eng. J.* **2016**, *285*, 27−38.
(39) Long, H.; Wu, P.; Yang, L.; Huang, Z.; Zhu, N.; Hu, Z. Efficient removal of cesium from aqueous solution with vermiculite of enhanced adsorption property through surface modification by ethylamine. *J. Colloid Interface Sci.* **2014**, *428*, 295−301.
(40) Sarier, N.; Onder, E.; Ersoy, S. The modification of Na-montmorillonite by salts of fatty acids: an easy intercalation process. *Colloids Surf. A Physicochem. Eng. Asp.* **2010**, *371*, 40−49.
(41) Tian, P.; Han, X.; Ning, G.; Fang, H.; Ye, J.; Gong, W.; Lin, Y. Synthesis of porous hierarchical MgO and its superb adsorption properties. *ACS Appl. Mater. Interfaces* **2013**, *5*, 12411−12418.
(42) Wan, D.; Wang, G.; Li, W.; Wei, X. Investigation into the morphology and structure of magnetic bentonite nanocomposites with their catalytic activity. *Appl. Surf. Sci.* **2017**, *413*, 398−407.
(43) Tanhaei, B.; Ayati, A.; Sillanpää, M. Magnetic xanthate modified chitosan as an emerging adsorbent for cationic azo dyes removal: Kinetic, thermodynamic and isothermal studies. *Int. J. Biol. Macromol.* **2019**, *121*, 1126−1134.
(44) Zhang, L.; Zhang, B.; Wu, T.; Sun, D.; Li, Y. Adsorption behavior and mechanism of chlorophenols onto organoclays in aqueous solution. *Colloids Surf., A* **2015**, *484*, 118−129.
(45) Li, X.; Wang, Z.; Ning, J.; Gao, M.; Jiang, W.; Zhou, Z.; Li, G. Preparation and characterization of a novel polyethyleneimine cation-modified persimmon tannin bioadsorbent for anionic dye adsorption. *J. Environ. Manage.* **2018**, *217*, 305−314.
(46) Park, Y.; Ayoko, G. A.; Horváth, E.; Kurdi, R.; Kristof, J.; Frost, R. L. Structural characterisation and environmental application of organoclays for the removal of phenolic compounds. *J. Colloid Interface Sci.* **2013**, *393*, 319−334.
(47) Yang, S.; Gao, M.; Luo, Z. Adsorption of 2-naphthol on the organo montmorillonites modified by Gemini surfactants with different spacers. *Chem. Eng. J.* **2014**, *256*, 39−50.
(48) Chen, D.; Chen, J.; Luan, X.; Ji, H. P.; Xia, Z. G. Characterization of anion-cationic surfactants modified montmorillonite and its application for the removal of methyl orange. *Chem. Eng. J.* **2011**, *171*, 1150−1158.
(49) Rawajfih, Z.; Nsour, N. Characteristics of phenol and chlorinated phenols sorption onto surfactant-modified bentonite. *J. Colloid Interface Sci.* **2006**, *298*, 39−49.
(50) Ruan, X.; Liu, H.; Chang, C.; Fan, X. Preparation of organobentonite by a novel semidry-method and its adsorption of 2,4-dichlorophenol from aqueous solution. *Int. Biodeterior. Biodegrad.* **2014**, *95*, 212−218.
(51) Huang, L.; Zhou, Y.; Guo, X.; Chen, Z. Simultaneous removal of 2,4-dichlorophenol and Pb(II) from aqueous solution using organoclays: Isotherm, kinetics and mechanism. *J. Ind. Eng. Chem.* **2015**, *22*, 280−287.
(52) Garmia, D.; Zaghouane-Boudiaf, H.; Ibbora, C. V. Preparation and characterization of new low cost adsorbent beads based on activated bentonite encapsulated with calcium alginate for removal of 2,4-dichlorophenol from aqueous medium. *Int. J. Biol. Macromol.* **2018**, *115*, 257−265.
(53) Muedas-Taipe, G.; Maza Mejía, I. M.; Santillan, Fátima A.; Velásquez, C. J.; Asencios, Y. J. O. Removal of azo dyes in aqueous solutions using magnetized and chemically modified chitosan beads. *Mater. Chem. Phys.* **2020**, *256*, 123595.
(54) Heinz, H.; Vaia, R. A.; Farmer, B. L. Interaction energy and surface reconstruction between sheets of layered silicates. *J. Chem. Phys.* **2006**, *124*, 224713.

https://doi.org/10.1021/acsomega.4c08924
ACS Omega 2025, 10, 10926−10937

(55) Wang, W. M.; Wu, P. X. Preparation of organic vermiculite and application for adsorption of 2,4-dichlorophenol from aqueous solutions. *J. Funct. Mater.* **2013**, *44*, 835−839.
(56) Yu, M.; Gao, M.; Shen, T.; Wang, J. Organo-vermiculites modified by low-dosage Gemini surfactants with different spacers for adsorption toward *p*-nitrophenol. *Colloids Surf. A Physicochem. Eng. Asp.* **2018**, *553*, 601−611.
(57) Ouachtak, H.; El Guerdaoui, A.; Haounati, R.; Akhouairi, S.; El Haouti, R.; Hafid, N.; Ait Addi, A.; Sljukic, B.; Santos, D. M. F.; Taha, M. L. Highly efficient and fast batch adsorption of orange G dye from polluted water using superb organo-montmorillonite: Experimental study and molecular dynamics investigation. *J. Mol. Liq.* **2021**, *335*, 116560.
(58) Xiang, Y.; Gao, M.; Ding, F.; Shen, T. The efficient removal of dimethyl phthalate by three organo-vermiculites with imidazolium-based gemini surfactants in aqueous media. *Colloids Surf. A Physicochem. Eng. Asp.* **2019**, *580*, 123726.

https://doi.org/10.1021/acsomega.4c08924
ACS Omega 2025, 10, 10926−10937